Mon. Not. R. astr. Soc. (1976) **175**, 1–24.

NEUTRAL HYDROGEN IN THE GALACTIC CENTRE REGION—II

Location of the Emission Features

R. J. Cohen and R. D. Davies

University of Manchester, Nuffield Radio Astronomy Laboratories, Jodrell Bank, Macclesfield, Cheshire SK11 9DL

(Communicated by the Director, Nuffield Radio Astronomy Laboratories)

(Received 1975 October 30; in original form 1975 October 2)

SUMMARY

An interpretation and discussion is given of Cohen's observations of 21-cm hydrogen line emission from the galactic centre region. Only the high-velocity emission distinct from the main maximum at zero velocity is considered. The distances of many of the individual emission features have been estimated from the variation of velocity with longitude, and these distances used to calculate hydrogen masses and the z-distances of the gas above and below the plane. The distribution of gas within 2·5 kpc of the centre is found to be tilted with respect to the plane, with its pole in the direction $l = 124 \pm 28°$, $b = 81 \pm 4°$. Expansional components of motion of up to 175 km s^{-1} away from the centre are found, with a tendency for higher expansion velocities to occur nearer the centre. The rotational velocities of features lying out of the plane are found to decrease markedly towards the centre. These rotational velocities are considerably less than the circular velocities given by the Rougoor–Oort rotation curve. On the other hand the rotational velocities of the features in the disk follow this curve quite well for distances between 4 and 2 kpc from the centre, and again within about 800 pc of the centre. These results are discussed in terms of two current theories on the origin of non-circular motions in the central region of the Galaxy.

1. INTRODUCTION

The study of the central region of our Galaxy is important firstly because we are able to study the Galaxy in far greater detail than nearby galaxies, and secondly because activity has been observed there which may be related to the origin of spiral structure. Much of our knowledge of this region has come from observations of the 21-cm transition of neutral hydrogen (H I). The pioneering observations made at Dwingeloo revealed emission over a wider range of radial velocities (normally measured relative to the local standard of rest, lsr) than found anywhere else in the Galaxy. The emission with the highest velocity is seen in a thin layer very close to the centre, with negative velocity at negative galactic longitude and positive velocity at positive longitude (Rougoor & Oort 1960). This indicates rapid rotation of gas near the galactic centre, and implies a concentration of mass in the nucleus, which has been confirmed by infrared observations (Becklin & Neugebauer 1968). At lower velocities there are a number of emission features having the appearance of spiral arms, whose velocities change more slowly with

longitude. The brightest of these is the well-known 3 kpc arm, which can be traced over 30° of longitude, from its tangential point at longitude $l = 336°$ to $l = 6°$ where its profile blends with the main maximum of emission near zero velocity.

The surprising fact about these innermost arms is that their line-of-sight velocities do not drop to zero at zero longitude. Therefore the arms cannot be in simple rotation, but must possess large non-circular components of motion of the order of 100 km s^{-1}. These are usually interpreted in terms of a general expansion in the inner region of the Galaxy. By assuming an axially symmetric field of expansion and rotation velocities, Rougoor (1964) could account for the observed velocities of the emission, and locate individual features along the line of sight according to their velocities. However, Rougoor's data appeared to show an asymmetry between the emission at positive and negative velocities, and in order to explain the absence of emission at velocities predicted by the axisymmetric model he had to assume gas to be almost entirely absent from some regions. Rougoor suggested an explosion in the nuclear region as one possible source of both the expansion of gas and the irregularity in its distribution. The salient points of this interpretation have been very clearly outlined by Oort (1964).

More recent observations by Kerr (1967), van der Kruit (1970), Sanders, Wrixon & Penzias (1972) and Cohen (1975) have revealed extensive emission lying well out of the galactic plane, with non-circular velocities similar to those of the arms in the plane. In the light of these observations it is now clear that much of the asymmetry between positive and negative velocity emission in Rougoor's maps was due to the limited latitude range of his survey. Fig. 1 taken from Paper I of this series (Cohen 1975) shows the ridge lines in the longitude–velocity (l–V) plane of all the high-velocity emission features detected in the Jodrell Bank survey, covering the region between longitudes 355 and 10° and between latitudes ±5°. It is apparent that, when emission over this wider range of latitude is taken into account, much of the symmetry of the l–V diagram about its origin $l = 0°$, $V = 0$ is restored.

In the present paper we consider the problem of locating the high-velocity hydrogen along the line of sight. Many of the features are arm-like, and their velocities can be explained by a simple model which is described in Section 2. This analysis yields information about the gas distribution and kinematics in the central region. The coherent picture we obtain is one of the main justifications for the simple assumptions involved. In Section 3 the results are discussed in relation to current theories on the origin of the large non-circular motions seen in the direction of the centre. The explosion theory has been treated in detail by van der Kruit (1971a), and applied to the active galaxy NGC 4258, where it has been suggested that we are witnessing the birth of major spiral arms (van der Kruit, Oort & Mathewson 1972). An interesting alternative explanation of the non-circular motions in our own Galaxy has been offered by Shane (1972) and by Simonson & Mader (1973). They have shown that some of the brightest features can be explained if the gas moves in elliptical orbits such as are predicted to occur near the inner Lindblad resonance (Contopoulos 1970). In this case the expansion velocities observed at $l = 0°$ are only an apparent effect due to the orientation of the ellipses, and there is no net outflow of matter. Although our results shed new light on both these theories, it does not appear possible to distinguish between the two on the basis of the present observations.

Further 21-cm line observations which may help to resolve this problem have

been made with the Mark IA radio telescope (beam 13′), and will be presented in subsequent papers in the series. Paper III will describe H I absorption measurements of the nuclear continuum sources, and Paper IV will describe H I emission associated with the nucleus, in particular the nuclear disk feature, and the molecular ring at ~250 pc from the centre.

2. THE LOCATION OF THE EMISSION FEATURES

2.1 *A simple model*

From an inspection of Fig. 1 it is apparent that most of the ridge lines in this l–V diagram have similar characteristics, namely velocity gradients in the sense expected from differential galactic rotation, plus large non-circular velocities at zero longitude. As the starting point for our analysis we consider the simplest axially symmetric model which can account for these properties. This is the so-called expanding and rotating ring. To a first approximation, we suppose that a feature such as the 3-kpc arm can be represented as a circular arc centred on the galactic nucleus, and undergoing both rotation and radial expansion. If the circle is of radius a, and the arm has a rotational velocity V_R and a velocity of expansion V_E, then the line-of-sight velocity with respect to the lsr is given as a function of galactic longitude by the expression

$$V_{LSR} = \left(\frac{r_0}{a} V_R - U_0\right) \sin l \pm \left(1 - \frac{r_0^2}{a^2} \sin^2 l\right)^{1/2} V_E, \qquad (1)$$

where r_0 is the distance of the Sun from the galactic centre, and U_0 is the rotational velocity of the lsr about the centre. The values $r_0 = 10$ kpc and $U_0 = 250$ km s^{-1} have been assumed in the following analysis. We see from equation (1) that for a given longitude l there are two possible values of V_{LSR}, corresponding to the far and near sides of the ring, and also that the same functional dependence of V_{LSR} on l is obtained with negative values of V_E. That is, the kinematics alone do not enable one to distinguish between expansion and contraction of the ring.

Rougoor (1964) fitted such a model to his observations of the 3-kpc arm. For this arm there is direct observational evidence that the non-circular component of motion seen at $l = 0°$ is directed away from the galactic centre. This comes from the absorption spectrum of the radio continuum source in the galactic nucleus. The 3-kpc arm is seen in absorption against the continuum and so must lie on the near side of the centre, whereas the positive velocity features I, II and XVI which lie along the same line of sight are not seen in absorption and must lie beyond the centre. Therefore the ambiguity between expansion and contraction does not arise for these features. The radius of the 3-kpc arm model is defined by the longitude at which the arm is seen tangentially, and the expansion velocity by the velocity observed at zero longitude. Given the radius a, the rotation velocity can be determined either from the velocity at which the arm is seen tangentially,

$$V_{tangent} = V_R - U_0 \frac{a}{r_0}, \qquad (2)$$

or from the velocity gradient at $l = 0°$:

$$\left.\frac{dV}{dl}\right|_{l=0°} = \frac{r_0}{a} V_R - U_0. \qquad (3)$$

1976MNRAS.175....1C

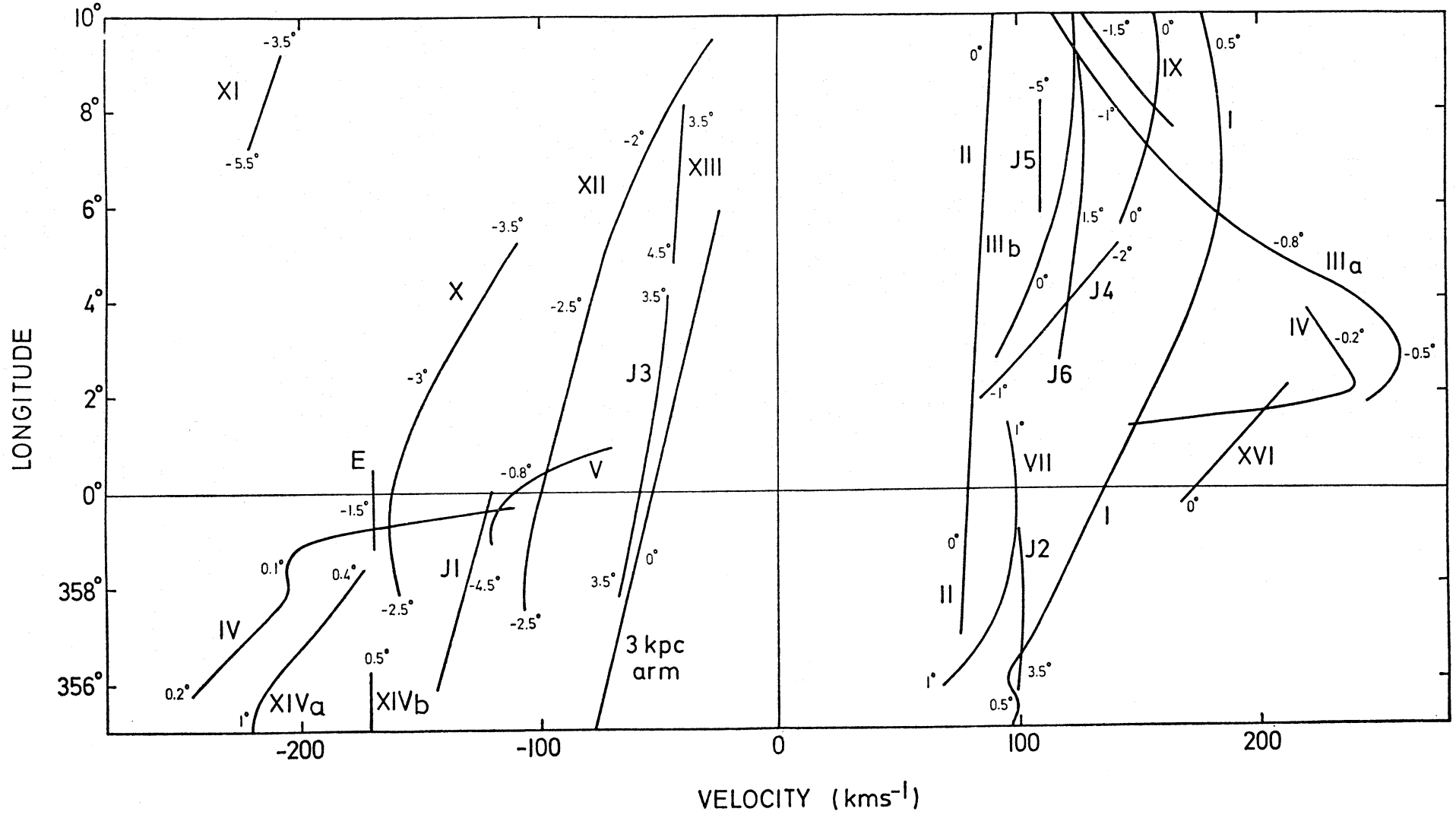

FIG. 1. *Longitude–velocity chart of high-velocity H I emission features detected in the Jodrell Bank survey of the galactic centre, reprinted from Paper I. Small numbers indicate the mean latitude of the emission. Note that the features XIV and XV have been relabelled XIVa and XIVb (see Appendix).*

The model obtained in this way by Rougoor gives an excellent fit to the velocity of the arm over the region of his survey ($l > -8°$). However, at more negative longitude the fit deteriorates towards the tangential point, suggesting that the arm is not a circular arc but a spiral (Burke & Tuve 1963).

In the following sections we describe the results of fitting such models to features with similar loci in the longitude–velocity plane.

2.2 *van der Kruit's feature XII*

We consider first van der Kruit's feature XII. This is the most extensive of the emission features lying out of the galactic plane. It covers an area of some $12 \times 5°$ beneath the galactic equator at a mean latitude of $-2°{\cdot}5$ and has been described in detail in Paper I. It was noted there that the velocity of the feature is smaller at low longitude than was found by Sanders & Wrixon (1972a) at lower resolution ($2° \times 16$ km s^{-1}). The reasons for this discrepancy are apparent from Fig. 2. Here we show the l–V map at $b = -4°$ obtained by Sanders & Wrixon, together with their best-fitting model for the feature, namely

$$a = 2{\cdot}4 \text{ kpc}, \quad V_R = 151 \text{ km s}^{-1}, \quad V_E = 128 \text{ km s}^{-1}, \tag{4}$$

the velocities for which are shown by a dotted line. The filled circles show the mean velocities of features XII, X and J1, obtained from the Jodrell Bank survey by averaging the velocity of each feature in latitude. That is, each point represents a weighted mean, with spectra at different latitudes being weighted according to the intensity of the feature. It is evident from Fig. 2 that the higher velocity assigned to feature XII by Sanders & Wrixon was due to confusion with the feature J1 which lies at a mean latitude of $-4°{\cdot}5$, within the $2°$ beam of their telescope.

Feature XII is not seen at its tangent point, so the radius of the ring and the rotational velocity are defined by the curvature of the l–V locus. The best-fitting model we obtain has parameters

$$a = 2{\cdot}4 \text{ kpc}, \quad V_R = 120 \text{ km s}^{-1}, \quad V_E = 99 \text{ km s}^{-1}, \tag{5}$$

and the velocities for this model are shown in Fig. 2 by a dashed line. The standard deviation of the fit is 2·7 km s^{-1}, which is less than the velocity resolution of the survey (7·3 km s^{-1}). The accuracy to which the model is defined by the fitting procedure can be estimated as follows. The sum of squares of the errors would double if the radius a were increased to 2·6 kpc or decreased to 2·3 kpc with the velocities kept constant, and similarly it would double if the rotational velocity were increased to 126 km s^{-1} or decreased to 111 km s^{-1} with a and V_E constant, or if the expansional velocity were increased to 103 km s^{-1} or decreased to 96 km s^{-1} with a and V_R constant.

Since feature XII does not extend to $l = 0°$, $b = 0°$ the absorption spectrum of Sgr A cannot be used as a test of whether it lies in front of or behind the centre. The kinematics alone do not distinguish an expanding ring from a contracting one either, and it is only when we consider the dynamics of expansion and contraction that it becomes possible to decide. This is because of the low rotational velocity of the feature, $V_R = 120$ km s^{-1}, which is only half the circular velocity (the velocity required to maintain the gas in a circular orbit of radius $a = 2{\cdot}4$ kpc). This is precisely the situation one would expect if the gas had been expelled from the nuclear region of the Galaxy.

To see why this is so, consider a particle in equilibrium in a circular orbit

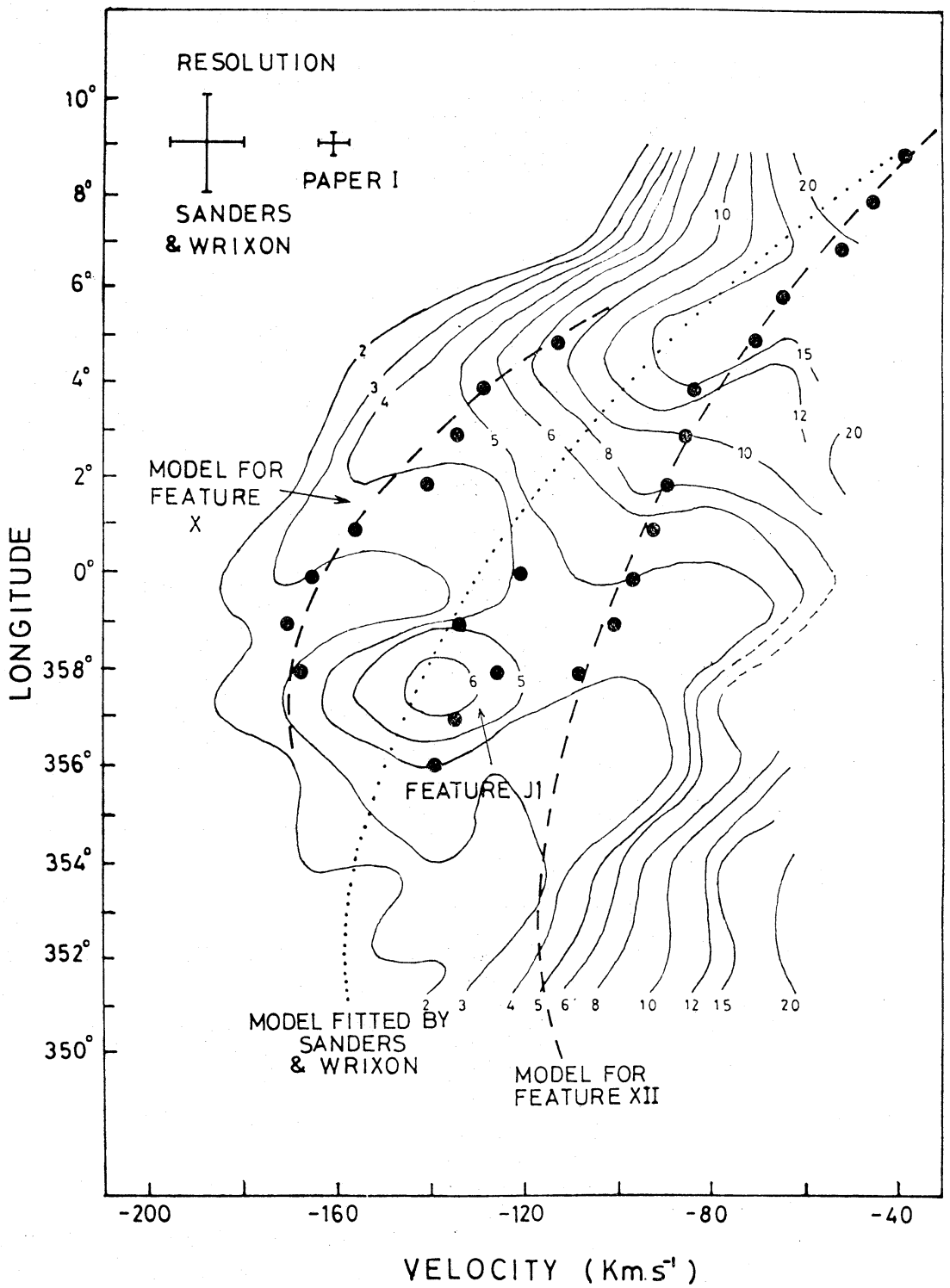

FIG. 2. *Longitude–velocity map at latitude $b = -4°$, taken from Sanders & Wrixon (1972a). The dotted line indicates their model velocities for feature XII, (4) in the text. Filled circles represent mean velocities for features X, XII and J1 obtained from the Jodrell Bank survey, and the dashed lines show the velocities of our best fits to features X and XII, described in the text. The fit by Sanders & Wrixon to feature XII is strongly influenced by emission from feature J1, and this is responsible for the discrepancy between our model and theirs.*

about the centre. If it is given a radial impulse outwards, and we neglect collisions, then its rotational velocity will fall inversely as the distance from the centre to conserve angular momentum. On the other hand, the circular velocity cannot fall as sharply whatever the distribution of matter in an axially symmetric model. Accordingly the rotational velocity of the particle must become steadily less than the circular velocity. In the same way an infalling particle must reach a higher rotation velocity than the circular velocity. Therefore we conclude from the low rotational velocity of feature XII that it originated near the nucleus, and is now being observed in expansion. The possibility that it is infalling from a region of low angular momentum outside the galactic disk is discounted by the absence of any velocity gradient with latitude.

This argues strongly that the feature is on the near side of the centre assuming an axially symmetric model. We will discuss in Section 3.2 below whether it should be interpreted in a more literal sense as evidence of an explosive event in the nucleus of the Galaxy.

2.3 *Other features described by the model*

The expanding and rotating ring model can be fitted in the same way to all the major emission features except the connecting arm (feature IIIa) and the nuclear disk (feature IV). The fits are of similar accuracy to that of feature XII, and define the model parameters to within 10 per cent. Our results are summarized in Table I, which appears in Section 2.6 below. All the rings are found to be expanding, either on the basis of H I absorption measurements as for the 3-kpc arm, or on the basis of the low rotational velocities as for feature XII. Therefore the location of these features in the galactic centre region is unambiguous under the assumption of axial symmetry.

A few remarks should be made about the fits to some of the individual features.

2.3.1 *Feature I* (' *the expanding arm at* $+135$ *km* s^{-1} '). It has been suggested by Sanders & Wrixon (1972a) that this feature and feature XII form part of a complete expanding and rotating ring structure 2·4 kpc from the galactic centre. Our model parameters for feature I are

$$a = 2{\cdot}2 \text{ kpc}, \quad V_R = 180 \text{ km s}^{-1}, \quad V_E = 137 \text{ km s}^{-1}, \tag{6}$$

in good agreement with those which Sanders & Wrixon obtained, namely

$$a = 2{\cdot}4 \text{ kpc}, \quad V_R = 170 \text{ km s}^{-1}, \quad V_E = 135 \text{ km s}^{-1}. \tag{7}$$

However, as discussed above, we find significantly lower rotation and expansion velocities for feature XII (*cf.* (5) above), and in view of this difference it seems unlikely that the two features belong to a continuous ring, although they are at similar distances from the centre. This conclusion is supported by the different angular structures of the two features, noted in Paper I. Feature I has a smooth and compact distribution of column density, whereas XII is patchy and more extended (*cf.* Table I below).

2.3.2 *Feature II.* This arm extends to positive longitudes well beyond the range of our survey, where it appears to divide into at least two branches (Burton & Shane 1970; Shane 1972). We have arbitrarily fitted to the innermost branch, although an equally good fit to our data can be obtained with a larger radius and a correspondingly higher rotation velocity.

2.3.3 *Feature IIIb.* A radius of 2·5 kpc is suggested for this feature by its tangential point at $l = 14°{\cdot}5$. However, for no choice of velocities could we obtain a satisfactory fit over the full extent in longitude, so the feature cannot be circularly symmetric. For the purpose of determining the hydrogen mass a mean distance of 12·5 kpc from the Sun was adopted.

2.3.4 *Feature XVI.* The longitude–velocity pattern of this small feature does not define the model parameters very well. The expansion velocity is given by the velocity observed at $l = 0°$, $V_E = 175$ km s^{-1}, but the velocity of rotation and the ring radius are defined only by the velocity gradient at $l = 0°$:

$$V_R . \frac{r_0}{a} = 1450 \text{ km s}^{-1}.$$

With such a high expansion velocity the feature might be expected to have relatively low angular momentum, and so the rotation curve should provide an upper limit to the velocity V_R, which gives an upper limit to the distance a. This upper limit is 1·6 kpc if we use the Rougoor–Oort rotation curve, or 1·4 kpc if the rotation curve is given by feature IX as discussed in Section 2.5.3. A lower limit to the rotational velocity can be derived from the highest observed velocity of the feature, $V_{LSR} = 210$ km s^{-1} at $l = 2°$. From equation (1) this gives $V_R > 130$ km s^{-1}, corresponding to $a > 0{\cdot}9$ kpc.

2.3.5 *Feature J1.* In the same way feature J1 can be shown to lie between 1·3 and 2·5 kpc from the galactic centre. However, there is no direct evidence to show on which side of the centre the feature lies. We have tentatively assumed that it lies on the near side of the centre, since, like features X and XII, it occurs at negative latitude and has a similar negative velocity.

2.4 *Systematic effects in the fitted parameters*

At this stage it is useful to note some important results which emerge from the model-fitting analysis. The first is the symmetry about the galactic centre which can now be seen between the features which lie on the far side of the centre above the galactic equator (I, VII and J6), and the features on the near side which lie beneath the equator (V, X and XII). As discussed in Section 3.1 the inclination to the equator shown by these features is part of a tilt of the whole distribution of neutral hydrogen in the inner region of the Galaxy.

Secondly, the model velocities vary systematically with distance from the galactic centre. In Fig. 3 we show this variation for the expansion velocity. The velocities of the bright features in the galactic disk (indicated by filled circles) are similar to those of the more diffuse features lying out of the disk (indicated by open circles). In general, higher expansion velocities occur nearer the centre. The rotational velocities are plotted against distance from the centre in Fig. 4, together with the Rougoor–Oort rotation curve (shown as a full line), and some velocities indicated by triangles which are discussed in Section 2.5.3. We see from Fig. 4 that the velocities of rotation of the arms in the galactic disk lie fairly close to the Rougoor–Oort rotation curve, whereas the rotational velocities of features lying out of the disk are much lower, and decrease towards the centre.

We have thus verified that the velocity of gas varies with distance from the centre in qualitatively the same way as proposed by Rougoor (1964) in his model 4 for the velocity field, namely increasing expansion and decreasing rotation towards

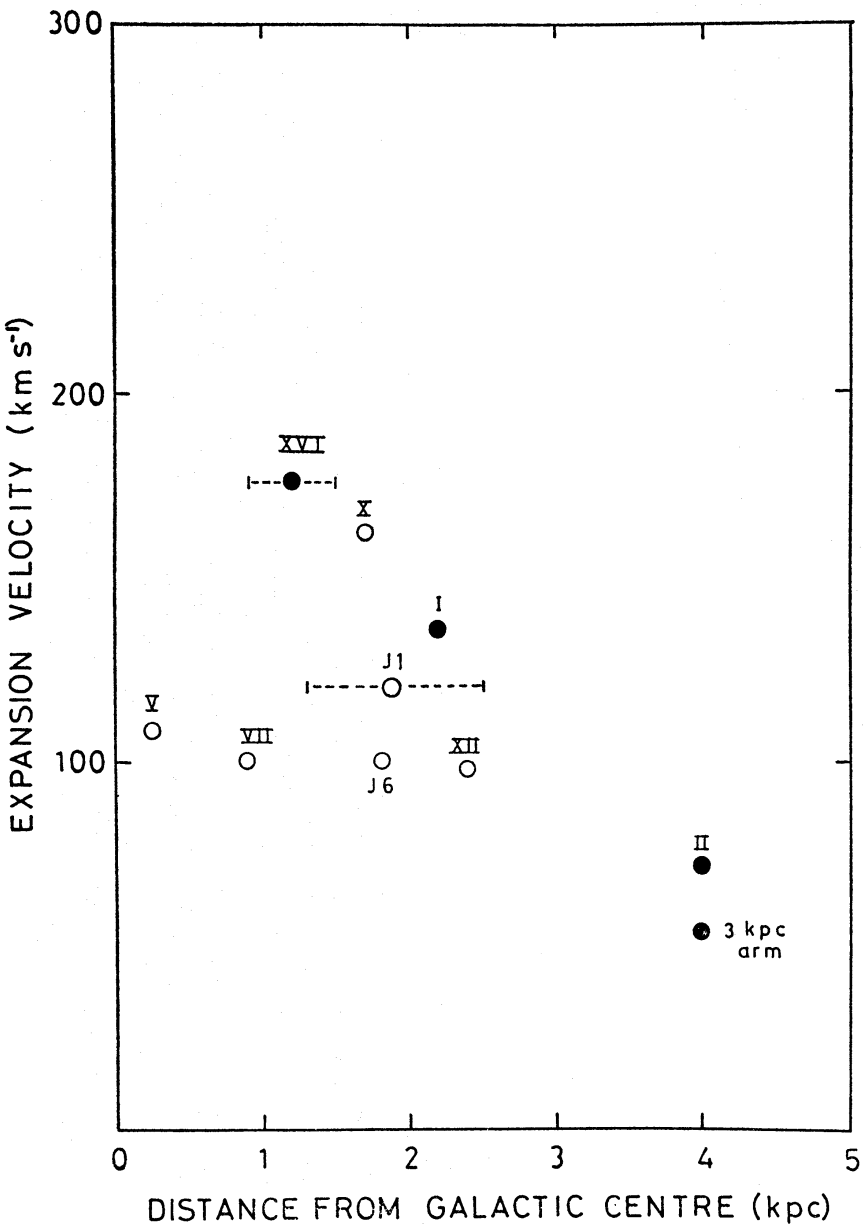

FIG. 3. *Expansion velocity plotted as a function of distance from the galactic centre, for H I emission features whose velocities have been fitted by the expanding and rotating ring model (Sections 2.1–2.3). Filled circles represent features in the galactic disk, and open circles represent features lying out of the disk. The 3-kpc arm and features V, X, XII and J1 lie on the near side of the centre, and the remaining features lie on the far side of the centre.*

the nucleus. However, Figs 3 and 4 also illustrate the difficulties involved in assigning an overall velocity field which is axially symmetric. The velocities plotted were derived assuming axial symmetry of the individual features, and this assumption is justified by the excellent fits obtained. Considered collectively on the other hand, the features do not exhibit the same degree of axial symmetry in their velocities. We find significant velocity differences between features at similar distances from the centre, such as X and J6, or I and XII. Evidently any axially symmetric model of the velocity field to encompass all the emission must oversimplify the true situation.

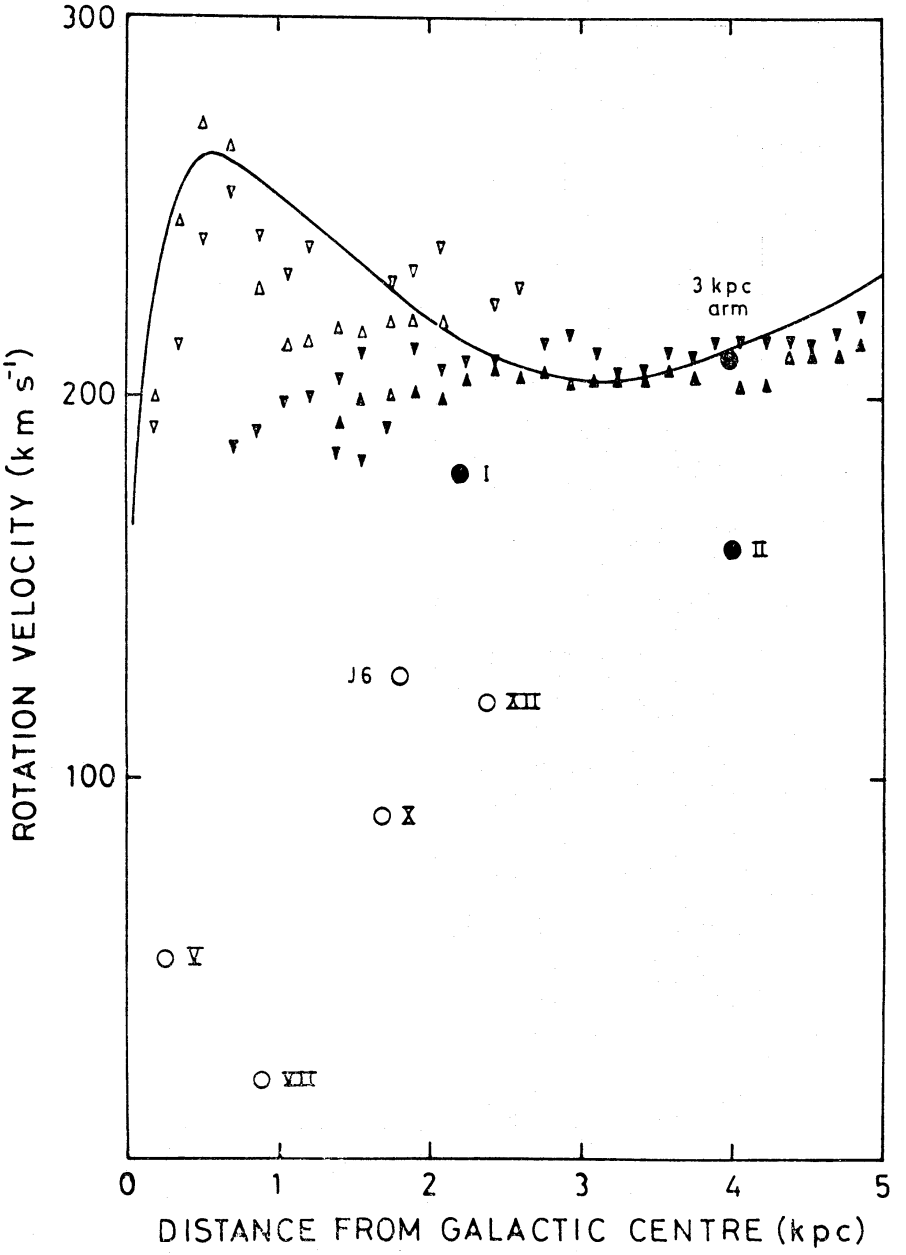

FIG. 4. *Rotation velocity plotted as a function of distance from the galactic centre, for H* I *emission features whose velocities have been fitted by the expanding and rotating ring model (Sections* 2.1–2.3*). Filled circles represent features in the galactic disk, and open circles represent features lying out of the disk. The* 3*-kpc arm and features V, X and XII lie on the near side of the centre and the remaining features lie on the far side of the centre. The Rougoor–Oort rotation curve is plotted as a solid line for comparison. The filled triangles show the rotation velocities of feature IX (upright triangles) and its counterpart feature XIVb at negative longitude (inverted triangles). These are the extreme velocity features in the disk for longitudes beyond* ±12°. *For smaller longitudes the extreme velocities, which are due to other features, are shown as open triangles to complete the figure. Data for the regions not covered by the Jodrell Bank survey have been taken from Kerr* (1969) *and Burton* (1970).

2.5 *The remaining features*

Of the features we have not discussed so far, several can be located in the nuclear region with certainty, whereas for others the data permit many interpreta-

tions. The distances we have adopted are given in Table I below (Section 2.6), and we will briefly explain how these were determined for individual features.

2.5.1 *Feature IIIa* (' *the connecting arm* '). This is the most problematical of the bright arms, and different interpretations of the feature have been discussed by Rougoor (1964), Kerr (1967) and van der Kruit (1970, 1971a). It is clear from the way the *l–V* locus runs counter to those of the other positive–velocity arms that this feature cannot be a spiral of small pitch angle. Rougoor's model for the field of velocities gives two possible locations for the feature, one on the near side and one on the far side of the centre. In both cases the feature has the appearance of a steeply inclined spiral. Kerr has interpreted the feature and its negative–velocity counterpart, feature XIVa, as forming a central bar in the Galaxy (a spiral of maximum pitch angle!), with IIIa on the far side of the centre and XIVa on the near side joining the 3-kpc arm. Van der Kruit (1971a) on the other hand has argued that IIIa is the result of a dip in the rotation curve, which could give rise to an emission feature without a gas density concentration along the line of sight, in the way explained by Burton (1971). Since we find the rotation curve feature discussed by Burton to connect smoothly with feature IX, it seems more natural to us to regard IX as the extension of Burton's rotation curve feature to lower longitudes, and to seek an alternative explanation for feature IIIa. There is some evidence that IIIa and XIVa form part of a single bar-like structure, as they have similar *l–V* loci and velocity profiles, and appear on the sky symmetrically disposed about the nucleus: IIIa lies beneath the galactic equator at positive longitude and XIVa lies above the equator at negative longitude. The observations provide no strong evidence for the orientation of such a bar: the apparent conjunction of feature XIVa and the 3-kpc arm noted by Kerr (1967) may be purely a line of sight effect and the different halfwidths in latitude of the two features indeed suggest that they are located at different distances. We believe there is a strong argument for placing the bar orthogonal to the orientation Kerr suggests, so that IIIa is then on the near side of the centre and the bar follows the inclination we have found above for features described by expanding rings.

2.5.2 *Feature IV* (' *the nuclear disk* '). The interpretation of this feature as a disk of gas in rapid rotation about the galactic nucleus was first made by Rougoor & Oort (1960). They concluded that rotational motion must predominate over radial motion in the disk, and the analysis by Rougoor (1964) was based on the assumption of pure rotation. However, observation of this feature near zero longitude, where radial motion will become most apparent, is hampered by absorption effects and by confusion with emission at lower velocities, and the observations published to date certainly do not rule out the possibility of a radial component of motion of the order of 100 km s^{-1}. We will therefore postpone further discussion until Paper IV of this series, where we present high resolution observations of the central part of the disk taken with the MK IA telescope.

2.5.3 *Feature IX*. At positive longitudes, beyond the limit of the Jodrell Bank survey, feature IX is the extreme positive–velocity feature. Burton (1971) has shown, using his technique of constructing model profiles from an assumed density and velocity distribution, that such a feature arises naturally, even in uniform density models, from the geometrical fact that at a given longitude the velocity of gas near the tangential point changes very slowly along the line of sight. The rotational velocity of feature IX is shown in Fig. 4 by filled triangles, and that of the corresponding negative–velocity feature by inverted filled triangles. The velocities

of the two are in good agreement, and follow the Rougoor–Oort curve quite well for distances greater than 2 kpc from the centre. Nearer the centre they depart from the curve, suggesting that the rotational velocity of gas is lower here. The open triangles in Fig. 4 have been plotted to complete the figure. They correspond to the extreme velocities seen at lower longitudes where the extreme velocity is no longer due to feature IX or its negative–velocity counterpart. These are the velocities one would naively use to define a rotation curve, but they do not necessarily indicate the rotational velocity of the gas. For example the positive–velocity points from $l = 6°$ to $l = 11°$ are due to feature I, which is known to have a large non-circular component of motion.

2.5.4 *Feature XI.* The distance to this small feature is very uncertain. Saraber & Shane (1974) have considered three possible interpretations of the feature, none of which can be ruled out by the observations. There is circumstantial evidence that the feature lies in the galactic centre region since it occurs at negative latitude with negative velocity, following the brighter features V, X and XII whose distances we know from the model-fitting analysis. Apart from this, the observed properties of the feature do not distinguish it from high-velocity clouds seen in many other directions in the Galaxy.

2.5.6 *Feature XIII.* We have no evidence on the distance to this feature, beyond the suggestion by Simonson (1971) that it is associated with the 3-kpc arm, and it is equally possible that the feature is not located in the centre region at all.

2.5.7 *Feature E.* Because of the large non-circular velocity of this feature, its broad profile, and its occurrence at zero longitude, it is possible that the feature is being expelled from the nuclear region. This conclusion is supported by the negligible change of velocity with longitude for the feature, which implies low angular momentum. Furthermore, feature E is seen beneath the plane with a negative velocity, in common with features V, X and XII which we know to be on the near side of the centre and expanding away from the centre region.

2.5.8 *Feature J2.* This feature also seem to be connected with the nuclear region, on account of its geometrical alignment. Sanders & Wrixon (1972b) have suggested that the H I emission is associated with the steeply inclined 20-cm continuum ridges found by Kerr & Sinclair (1966) which point directly at the feature. In this case it is hard to understand why no symmetric counterpart to J2 is seen in the opposite *l–b* quadrant. The claim by Sanders & Wrixon that feature E is such a counterpart must be treated with caution since it is likely, as noted in Paper I, that the extension of feature E towards positive longitude which these authors observed was due to confusion with feature X. Furthermore the profile halfwidths and velocities of E and J2 are dissimilar.

2.5.9 *Feature J4.* A more impressive geometrical alignment is displayed by feature J4, whose ridge of emission points directly away from the galactic centre at an angle of 20° with the equator. This well-defined angle and the very broad profile of the emission suggest that the gas is being expelled from the nuclear region. The projected line-of-sight velocity at zero longitude is small, implying that the expulsion is nearly transverse to the line of sight.

2.5.10 *Feature J5.* It is possible that this small feature may also have been expelled from the nucleus, since it lies on the ridge of positive–velocity emission defined by J2 and J4 (see Fig. 6 below), but we have no further evidence for its distance.

2.6 *Hydrogen masses*

Having estimated a distance D kpc for each emission feature, we can now calculate the hydrogen mass from the observed column density $N_{\mathrm{H\,I}}\mathrm{cm}^{-2}$, using the formula

$$\frac{m_{\mathrm{H\,I}}}{m_\odot} = 2{\cdot}43 \times 10^{-18}\, D^2 \int N_{\mathrm{H\,I}}\, dA, \qquad (6)$$

where the element of area dA is in units of square degrees. The masses are given in Table I, which provides a summary of our results.

With only one exception the masses have been evaluated over the region $-5^\circ \leqslant l \leqslant 10^\circ$, $-5^\circ \leqslant b \leqslant 5^\circ$. That is, we have not attempted to estimate the total masses of features extending beyond the limits of our survey. The exception is the 3-kpc arm. In this case we have used our data for the region $-5^\circ \leqslant l \leqslant 0^\circ$, where the emission from the arm is clearly distinguished, to estimate the mass of a full quadrant of the arm, following the calculation made by Rougoor (1964). He derived a mass of $2 \times 10^7\, M_\odot$ for the arm. The larger mass which we find can be attributed to the extended component described in Paper I, which has a z half-thickness perpendicular to the plane of ≈ 600 pc.

A useful quantity in comparing the relative importance of features is the mass per unit length. This can be calculated readily from the data in Table I. For the 3-kpc arm we find a mass per unit length of $5{\cdot}8 \times 10^6\, M_\odot\,\mathrm{kpc}^{-1}$, which can be compared with values of 2·2, 0·4, 1·7 and $0{\cdot}7 \times 10^6\, M_\odot\,\mathrm{kpc}^{-1}$ for features I, II,

TABLE I

Derived properties of galactic centre H I emission features

	Model parameters						
	a (kpc)	V_R (km s^{-1})	V_E (km s^{-1})	D (kpc)	Mean z (pc)	$\Delta z_{1/2}$ (pc)	$m_{\mathrm{H1}}/m_\odot$
3-kpc arm	4·0	210	53		0	178	$3{\cdot}6 \times 10^7$*
I	2·2	180	137		85	197	7×10^6
II	4·0	160	73		0	131	$1{\cdot}2 \times 10^6$
IIIa				8 → 10	−140	105 → 210	$\sim 2{\cdot}4 \times 10^6$
IIIb				12·5	0	213	$2{\cdot}6 \times 10^6$
IV				10	0	87 → 210	$1{\cdot}8 \times 10^6$†
V	0·25	52	107		−140	55	2×10^4
VII	0·9	20	100		183	~220	2×10^6
IX				10	0	123	6×10^5
X	1·7	90	162		−436	~145	7×10^4
XI				10?	−880	~175	$1{\cdot}7 \times 10^4$
XII	2·4	120	99		−330	~400	$1{\cdot}4 \times 10^6$
XIII				10?	610	105	7×10^4
XIVa				10 → 13	100 → 200	~200	5×10^5
XVI	$0{\cdot}9 < a < 1{\cdot}5$		175		0	77	3×10^5
E				10	−260	~350	6×10^4
J1	$1{\cdot}3 < a < 2{\cdot}5$		120		−640	85	$\sim 5 \times 10^4$
J2				10	520	~180	3×10^4
J3	Associated with 3-kpc arm			6	370	75	$1{\cdot}7 \times 10^4$
J4				10	−175	~70	$> 10^5$
J5				10?	−790	~175	$\sim 7 \times 10^4$
J6	1·8	127	100		310	310	$4{\cdot}4 \times 10^5$

* Estimated for a full quadrant of the arm, from our data in the range $-5^\circ < l < 0^\circ$.
† Estimated from the negative velocity wing, assuming a symmetric disk.

IIIb and XVI respectively, which lie in the disk on the opposite side of the centre. Comparable values of 1·4 and 0·7 × 10^6 $M_\odot$ kpc^{-1} are found for the brightest of the features lying out of the disk, features VII and XII respectively.

The relative masses of features can also be gauged from Fig. 5, which shows a

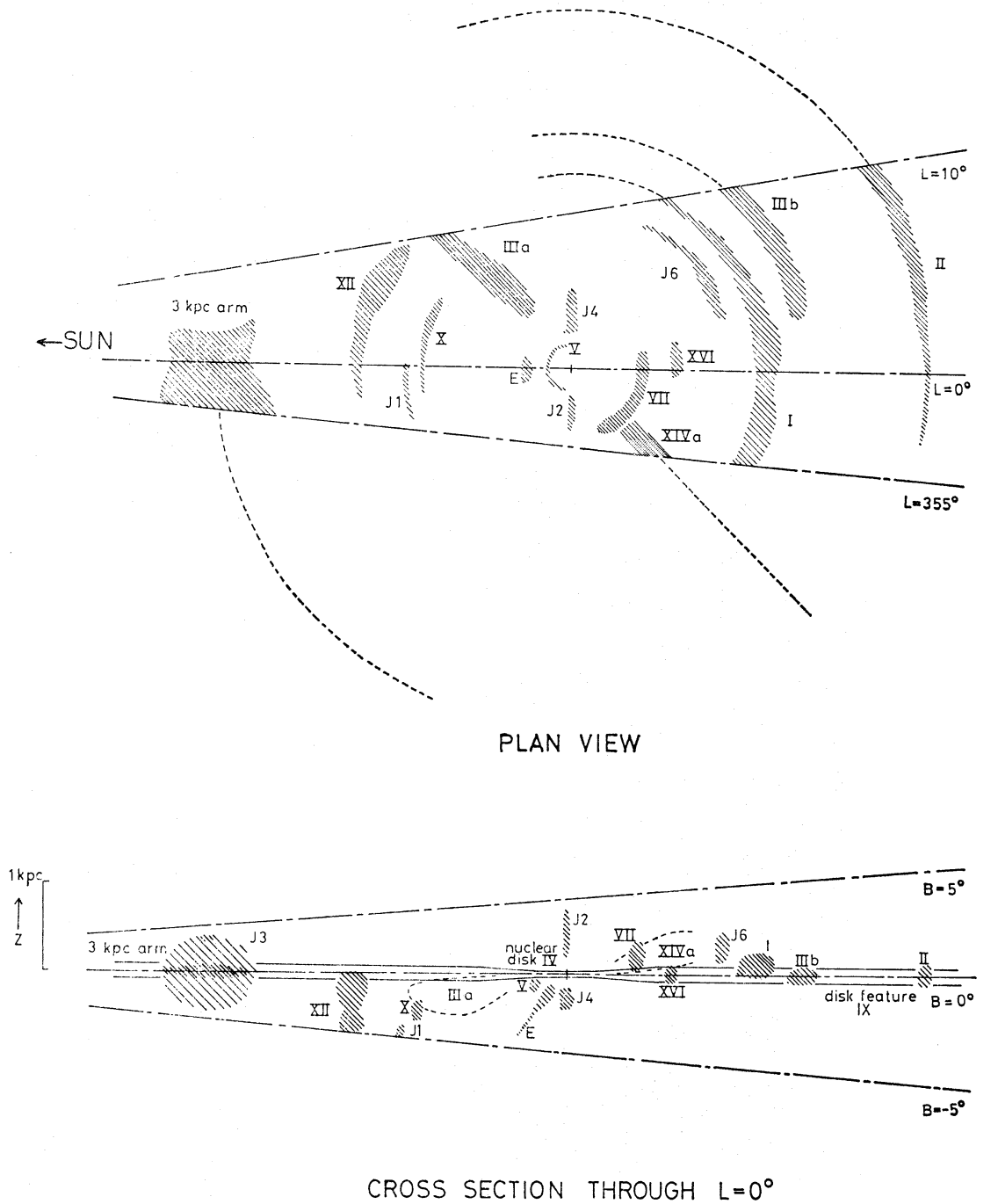

FIG. 5. *Possible location of H* I *emission features in the galactic centre, derived from the model-fitting analysis. The thickness of each feature is shown proportional to the peak column density, and corresponds to a uniform density of* 1 *H atom cm*$^{-2}$. *The dashed lines in the plan view show the full extent over which the brightest features can be seen, beyond the limits of our survey. The lower half of the figure illustrates the z distribution of the features. Here the approximate outline of the two bar features has been indicated by dashed lines. An outline of the classical galactic disk is also shown.*

schematic view of the galactic centre region with features located at the model distances derived above. Features XVI and J1, for which only limits to the distances are known, are shown at the mean of the two distances in each case. Features E, J2 and J4, which must lie in the vicinity of the centre, are shown at an arbitrary distance of 500 pc, and three of the smaller features with uncertain distances are not shown at all. The thickness of each feature is shown proportional to the peak column density, corresponding to an arbitrary volume density of 1 H atom cm^{-3}. Following the work of Burton, one should recognize that spectral features need not correspond to density enhancements at the model distances, but could be the result of velocity disturbances in these regions. This would not affect our conclusions on the mean distance and velocity of the gas. For a density of the order of 0·2 cm^{-3} the features would merge into a continuous distribution. The upper part of Fig. 5 is a plan view of the centre region, and its appearance strongly reflects our initial assumption of axial symmetry. The mean distances assigned to features cannot be too much in error, however, because of the accuracy of the fits to the circular model. The lower part of the figure is a cross-section through the line $l = 0°$, showing the z distribution of the gas. The inclination to the equator of features out of the plane is well illustrated by this diagram, and is seen to extend to distances of about 2·5 kpc from the centre.

To summarize, the main results of the model-fitting analysis are the following:

(i) A new symmetry about the centre is shown by the emission features lying out of the disk. The features lie above the plane on the far side of the centre, and beneath the plane on the near side of the centre.

(ii) There is a tendency for higher expansion velocities to occur nearer the centre.

(iii) The features out of the disk have very low rotation velocities, decreasing towards the centre.

3. DISCUSSION

3.1 *Tilt of the H I distribution near the centre*

The high-velocity emission we have been considering shows symmetry about the galactic centre in two ways. The first is in its distribution on the sky. The emission with the highest positive and negative velocities is disposed symmetrically about $l = 0°$, $b = 0°$, but with an inclination to the galactic equator of some 8°, as noted by Kerr (1967). This inclination is principally due to the bar features IIIa and XIVa, but the nuclear disk feature IV also shows a significant tilt in the same sense, at an angle of 4°. At intermediate velocities the emission features lying out of the plane have a marked inclination in the same sense. A good example is the ridge of positive-velocity emission formed by features J2, J4 and J5, shown in Fig. 6. A more surprising result which can be seen from this figure is that within a few degrees of zero longitude the main ridge of emission is also inclined to the equator, at about the same angle that Kerr found for emission at a much greater velocity. Many more examples of this tilt can be seen in individual features, and indeed it appears to be a general property of high-velocity emission from the galactic centre region. This result was given qualitatively in Paper I, and can be established quantitatively in the following way.

We consider emission from the symmetric region $-5° < l < 5°, -5° < b < 5°$ covered by the Jodrell Bank survey, and evaluate the centroid and angle of inclina-

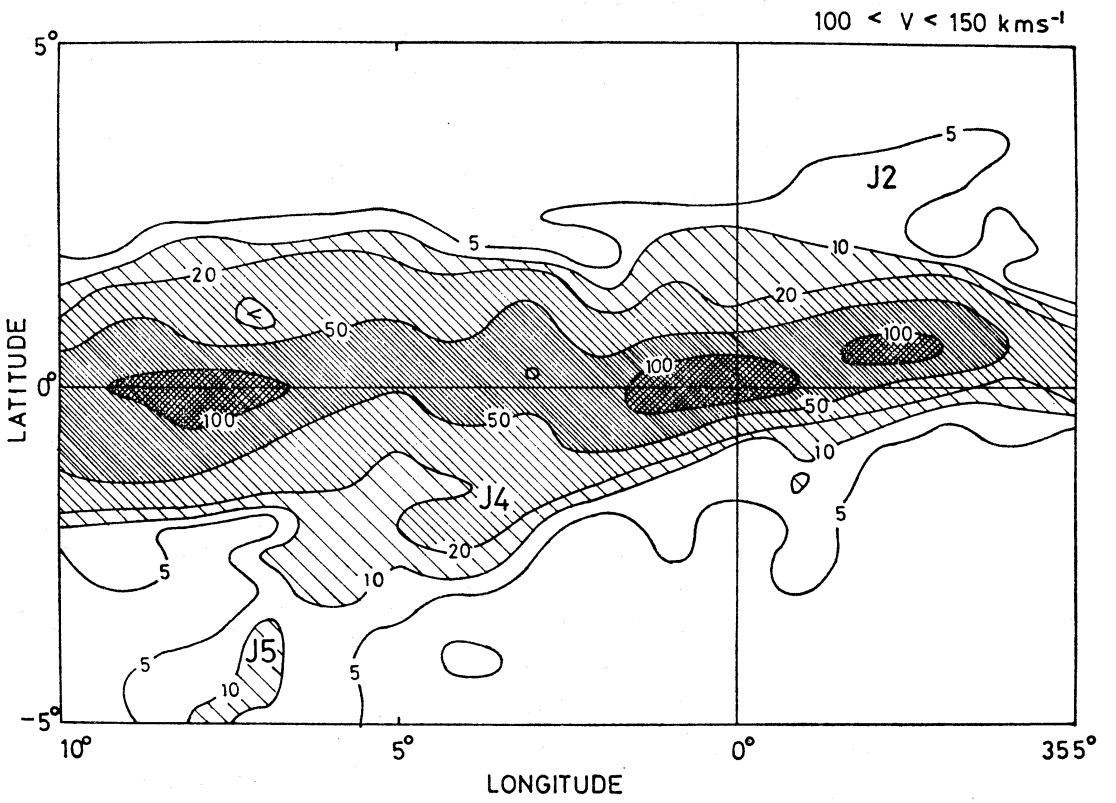

FIG. 6. *Column density of positive-velocity H I in the range* $100 < V < 150$ *km s*$^{-1}$, *showing the inclination to the equator of the bright emission near the plane and the striking ridges of emission lying out of the plane. The contour unit is* 10^{19} *atom cm*$^{-2}$.

tion of the distribution of H I column density, for each 50 km s^{-1} interval of velocity from $-300 \rightarrow -250$ km s^{-1} to $-100 \rightarrow -50$ km s^{-1}, and from $+50 \rightarrow +100$ km s^{-1} to $+250 \rightarrow +300$ km s^{-1}. This covers most of the emission which is distinct from the main maximum at zero velocity. If all this gas were located at a distance of 10 kpc from the Sun then its total mass would be $3 \times 10^7 M_\odot$. The centroids and angles are listed in Table II. The zero order moment μ_0 and the

TABLE II

Centroids and inclination angles of H I emission from the region $-5° \leqslant (l, b) \leqslant 5°$

Velocity range (km s^{-1})	$\bar{l}$ (°)	$\bar{b}$ (°)	μ_0 (10^{20} cm^{-2} deg^2)	θ (°) (°)
$-300 \rightarrow -250$	−3·5	0·0	2·8	−7·9 ± 3·6
$-250 \rightarrow -200$	−3·1	−0·2	28·7	−7·8 ± 4·5
$-200 \rightarrow -150$	−2·4	−0·2	61·4	−12·2 ± 9·7
$-150 \rightarrow -100$	−1·4	−0·7	105·0	−20·1 ± 6·7
$-100 \rightarrow -50$	−1·5	−0·1	396·7	−7·5 ± 1·2
$50 \rightarrow 100$	0·1	0·1	311·4	−9·7 ± 1·2
$100 \rightarrow 150$	0·7	0·2	177·5	−5·0 ± 0·7
$150 \rightarrow 200$	2·4	−0·1	93·9	−4·7 ± 1·2
$200 \rightarrow 250$	3·2	−0·5	42·8	−7·8 ± 2·7
$250 \rightarrow 300$	2·8	−0·6	8·7	−12·9 ± 5·3

centroids $\bar{l}$ and $\bar{b}$ are given by the equations

$$\mu_0 = \int N_{\mathrm{H\,I}}\, dA, \quad \bar{l} = \frac{\int N_{\mathrm{H\,I}} l\, dA}{\int N_{\mathrm{H\,I}}\, dA}, \quad \bar{b} = \frac{\int N_{\mathrm{H\,I}} b\, dA}{\int N_{\mathrm{H\,I}}\, dA},$$

and the angle of inclination θ to the galactic equator by the equation

$$\tan 2\theta = \frac{2\int N_{\mathrm{H\,I}}(l-\bar{l})(b-\bar{b})\, dA}{\int N_{\mathrm{H\,I}}(l-\bar{l})^2\, dA - \int N_{\mathrm{H\,I}}(b-\bar{b})^2\, dA},$$

where $N_{\mathrm{H\,I}}$ is the column density of gas emitting in the velocity range shown in the first column of the table. The last equation has two solutions for θ corresponding to the two principal axes of the distribution. The desired solution is the one which minimizes the ' moment of inertia ' of the distribution. From the rms noise level of the spectra and the baseline error, the rms error in μ_0 is estimated to be $0{\cdot}6 \times 10^{20}$ cm^{-2} deg^2. This is appreciable only for the two extreme velocity ranges where the emission is weakest, but the noise could lead to larger errors in the calculated centroids and angles of inclination since noise at the edge of the map will be heavily weighted. To reduce this effect only emission with a column density of greater than 2×10^{19} cm^{-2} was considered in evaluating the integrals. The integrals of negative-velocity emission are uncorrected for absorption against the nucleus.

The results are plotted in Fig. 7 with the centroids shown as they appear on the sky, and the angle θ indicated by an inclined line. It is immediately clear from this diagram that the inclination to the equator is similar at all velocities. The mean angle with the plane is $-7°{\cdot}4$, weighting each angle in the table inversely as the estimated error, and the standard deviation is $3°{\cdot}1$, this coming principally from one large angle. The mean angle agrees well with the angle of $-8°$ found by Kerr

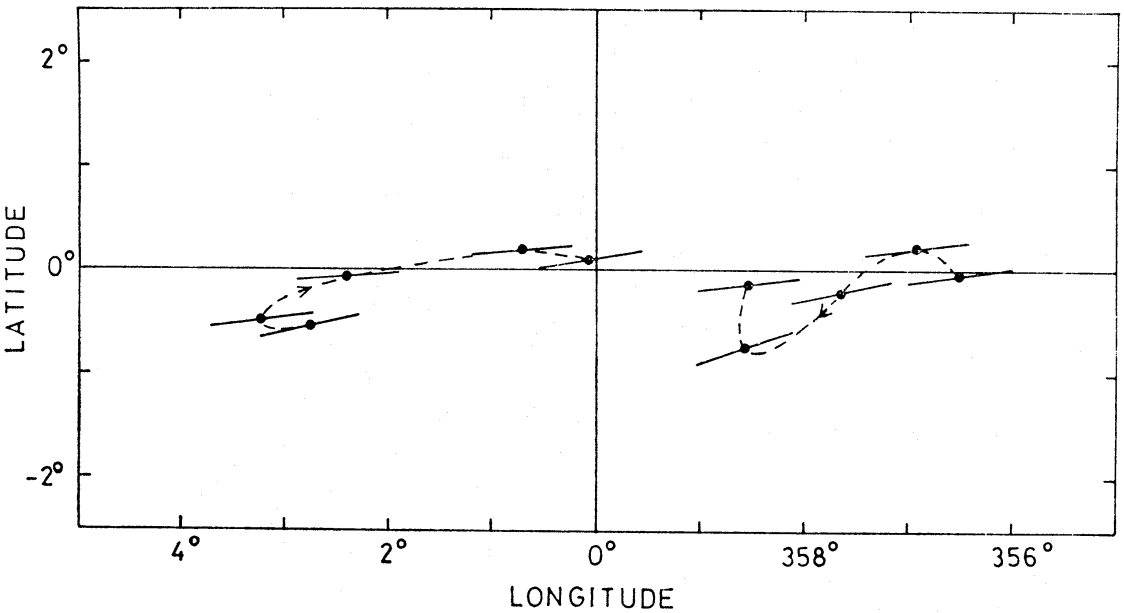

FIG. 7. *Centroids and first moments of high-velocity H* I *emission from the area* $-5° \leqslant l \leqslant 5°$, $-5° \leqslant b \leqslant 5°$, *evaluated in* 50 *km s*$^{-1}$ *intervals from* $(-300, -250)$ *to* $(-100, -50)$ *and from* $(50, 100)$ *to* $(250, 300)$. *The dashed lines and arrows show the direction from highest to lowest velocities. The negative-velocity moments are uncorrected for absorption against the nuclear continuum.* (*See also Table II.*)

(1967) for emission at the highest velocities.* This mean angle has been obtained directly from the observations and is independent of any assumption about the distribution of gas along the line of sight.

A further symmetry can be seen when distances are assigned by the model-fitting procedure described in Section 2. This is a symmetry about the centre shown by material lying out of the disk, which is clearly seen in the lower half of Fig. 5. Disregarding the small features E, J2 and J4, whose orientations in the nuclear region are uncertain, we see that material on the far side of the centre lies above the plane, and material on the near side of the centre lies beneath the plane. The tilt extends to a distance of about 2·5 kpc from the centre, and the angles with the plane range from 2°·2 for feature I to 29° for the small feature V. If one considers only the features with a well-defined tilt angle, which account for three-quarters of the observed high-velocity emission, then the mean angle defined is 5°·0.

The major part of the mass omitted in this calculation of the front-to-back (r–z) tilt resides in the nuclear disk feature IV. This feature follows the general l–b tilt on the sky, but although a front-to-back tilt of the disk is certainly consistent with the data, the evidence is less certain. Such a tilt would provide a simple explanation of the double structure in latitude seen in the intermediate-velocity emission at negative longitude. For example the b–V map at longitude $l = 356°$, presented in Paper I, Fig. 2(o), shows broad emission at ≈ -130 km s^{-1} which peaks in intensity at latitudes $+1°{\cdot}1$ and $-0°{\cdot}6$. This can be readily understood if the disk is tilted, for the front-to-back distance ambiguity is then resolved. A tilt in the disk might also remove the difficulty with the z-distribution of the gas, which appears far too great to be supported by the turbulent motions alone against the strong gravitational field in the nucleus (Sanders & Wrixon 1973). These matters will be pursued further in Paper IV.

Combining the front-to-back tilt angle with the tilt angle on the sky we can calculate the pole of the tilted gas distribution. This is in the direction $l = 124 \pm 28°$, $b = 81 \pm 4°$, taking the error in each measured angle to be 3°·1. There is an indication that the tilt may not be restricted to neutral hydrogen. The 20-cm continuum ridges mapped by Kerr & Sinclair (1966) display a symmetry in the same sense. In particular the main ridge line near $b = 0°$ is inclined at an angle of 7° with the equator, over the region within 2° longitude of the centre. A similar inclination to the equator can be seen on a smaller scale in the infrared maps at 2·2 μm presented by Becklin & Neugebauer (1968), especially in the most extensive map, taken with an aperture of 1′·8. Surveys of microwave molecular lines and hydrogen recombination lines from the galactic centre have been too poorly sampled in latitude to detect such a tilt, but we note that Kaifu, Iguchi & Kato (1974) report H I emission associated with the expanding and rotating molecular ring, and having a similar front-to-back tilt to that found here. If the molecular ring itself were symmetric about the galactic centre, its front-to-back tilt angle would be 8°.

3.2 *The explosion hypothesis*

Perhaps the most direct interpretation of the non-circular motions near the galactic centre is that we are observing an expulsion of gas from the nucleus. Our observations of gas lying out of the plane lend some support to this view, on

* Kerr considered only the outermost 70 km s^{-1} of emission, corresponding to velocities $|V| > \approx 180$ km s^{-1} for the longitude range we are considering.

account of the strong degree of symmetry about the centre shown by the gas, the low rotational velocities, and the high expansional components of motion directed away from the centre. van der Kruit (1971a) has calculated that such an expulsion of gas must have occurred at an angle of 25–30° with the plane. The constraints are that for a smaller angle of expulsion the rotating nuclear disk (feature IV) would have been swept up, while for a much larger angle the ejected gas would not have the high expansion velocity seen at present. In his interpretation the 3-kpc arm is the result of an expulsion some 12×10^6 yr ago, lasting several million years, and requiring $10^7\ M_\odot$ of gas to be ejected with velocities of ~ 600 km s^{-1}. The corresponding kinetic energy of the gas would be $\sim 4 \times 10^{55}$ erg. The material out of the plane can be explained only in terms of more recent activity some 5×10^6 yr ago involving some $10^6\ M_\odot$ of gas. Evidence for activity on a similar time scale is provided by the non-thermal radio continuum sources at the galactic centre, Sgr A and the extended source, whose lifetimes have been variously estimated at between 10^4 and 10^7 yr (Parijsky 1963; Downes & Maxwell 1966; Lequeux 1967). The energy in these sources in the form of electron kinetic energy and magnetic field energy is, however, several orders of magnitude less than the expulsion energy invoked by van der Kruit. Indeed, one uncomfortable aspect of the explosion theory is that it requires an unknown energy source in the nucleus.

The present observations place a number of constraints on possible expulsion mechanisms. The expanding and rotating ring models we have fitted define for each feature a characteristic age a/V_E and a mass flux $m_{H\,I}V_E/a$. These are given in Table III, together with the present kinetic energy of expansion $\frac{1}{2}m_{H\,I}V_E^2$. The wide range in ages and radial distances from the centre which we find suggests that expulsion has been a continual process, if not actually continuous. The total mass flux in the features is $1{\cdot}4\ M_\odot$ yr^{-1}, so that, allowing for gas moving transverse to the line of sight, the average outflow in the expansion model would be $\sim 3\ M_\odot$ per year. If one regards the nucleus as the seat of the expulsion one is then faced with the difficulty of accounting for this amount of interstellar gas (Rougoor & Oort 1960).

An upper limit to the initial distance of an expanding feature from the centre can be found from the model parameters if we project backwards in time and ask

TABLE III

Expansion parameters for H I emission features

	a (kpc)	$m_{H\,I}$ ($10^6\ M_\odot$)	Age a/V_E (10^6 yr)	Mass flux ($m_{H\,I}V_E/a$) (M yr^{-1})	Expansion energy ($\frac{1}{2}m_{H\,I}V_E^2$) (10^{50} erg)
3-kpc arm	4·0	36*	74	0·49*	10 000*
I	2·2	7†	16	0·44†	13 000†
II	4·0	1·2†	54	0·03†	640†
V	0·25	0·02	2	0·01	2
VII	0·9	2·0	9	0·23	2000
X	1·7	0·07	10	0·01	18
XII	2·4	1·4	24	0·06	1400
XVI	$0{\cdot}9 < a < 1{\cdot}5$	0·3	$5 \rightarrow 8$	$0{\cdot}06 \rightarrow 0{\cdot}04$	910
J1	$1{\cdot}3 < a < 2{\cdot}5$	0·05	$11 \rightarrow 20$	$0{\cdot}005 \rightarrow 0{\cdot}002$	8
J6	1·8	0·4	18	0·02	440

* Estimated for a full quadrant of the arm.

† Integrated only over the longitude range $-5° \leqslant l \leqslant 10°$.

at what distance from the centre would the feature have possessed the circular velocity, assuming conservation of angular momentum. In this way we find that features X, XII and J6 must have started within 1 kpc of the centre, and features V and VII within 100 pc of the centre. Projecting forwards in time we find that the features presently ≈ 2 kpc from the centre will not reach the distance of the 3-kpc arm before gravity pulls them back into the galactic disk, and features V and VII nearer the nucleus will fall even farther short. That is to say, successive expulsions of gas must have been less and less energetic. Finally, the distribution of expanding gas in an inclined plane suggests that expulsion must have been confined to a narrow range of angles over several rotation periods of the nuclear region.

As well as these constraints, the observations also introduce some difficulties with van der Kruit's model in which the ejected gas is braked by the interstellar medium as it falls back into the disk. In particular, it is hard to see why the most extensive features out of the plane, features XII and VII, do not show any velocity gradient with latitude. For example, feature XII is seen over more than 5° in latitude, corresponding to z-distances of 0 to -700 pc, and yet its velocity at $b = 0°$ where it is expected to be interacting with the disk is the same a sseen at $b = -5°$. This evidence, and the smooth variation of velocity with longitude, suggest that the feature is produced by some orderly process, rather than by sudden ejection and subsequent braking with relative velocities of ~ 200 km s^{-1} between the interacting gases. A similar argument can be made for most of the bright expanding features.

3.3 *Dispersion orbits and central bar*

The most promising alternative explanation of the non-circular motions is in terms of gravitational forces alone. In the density-wave theory of spiral structure the 3-kpc arm has been tentatively identified with the inner Lindblad resonance (Lin & Shu 1967). Following the calculations by Contopoulos (1970), Shane (1972) and Simonson & Mader (1973) have demonstrated that the elliptical orbits predicted for stars near the resonance can explain the observed velocities of the 3-kpc arm and of feature II, which they regard as the counterpart on the far side of the centre. Shane has determined the orientation of the ellipse to be towards $l = 152 \pm 10°$, with a mean radius of 4 kpc, a mean circular velocity of ≈ 210 km s^{-1} and an epicyclic velocity of 50–60 km s^{-1}. Similar values were found by Simonson & Mader. In this interpretation there is no net outflow of matter; indeed the dispersion ring would appear to be contracting when the pattern had rotated through one quadrant.

The calculations by Contopoulos show that resonance effects are restricted to a region within 1–1·5 kpc of the inner Lindblad resonance (i.e. ≈ 2–5 kpc from the galactic centre). Dynamical models for the region interior to this have not yet been developed, although Peters (1975) has shown that the velocities of the brightest features may be explained by a set of *ad hoc* nested elliptical orbits with axes parallel, such as might occur in the presence of a central bar. Such an interpretation is quite consistent with our observations which, indeed, remove one of the difficulties of Peters' work, namely the prediction of emission at positive longitudes with a velocity of ≈ -100 km s^{-1} which we see beneath the plane. In order to explain the highest expansion velocities, epicyclic motions of 100 km s^{-1} and axial ratios of 3:1 for the ellipses are needed. The orientations of the ellipses considered by Peters were in the directions $l = 135 \pm 15°$, coinciding within the errors with the direction we have found for the tilted gas distribution. This lends some support

to the view that the features might all be related to a central bar structure. It is clearly important to make dynamical calculations for the region interior to the Lindblad resonance to determine whether the orbits considered by Peters have a physical basis.

4 *Comparison with other galaxies*

Non-circular motions of the same order as seen in our own galactic centre are also seen in the nuclear regions of many nearby normal spiral galaxies (*cf.* the review article by G. R. Burbidge (1970)), and several show remarkable similarities in their kinematics to our galactic centre. The resemblance is particularly strong in the case of M31, the best studied example. Observations of optical emission lines show rapid rotation of gas near the nucleus, rising to ≈ 200 km s^{-1} at a distance of $R = 400$ pc from the centre, and falling to a deep minimum near $R = 2$ kpc (Rubin & Ford 1970, 1971). The small velocity dispersion of the gas suggests that it is concentrated in a thin rotating disk (Rubin & Ford 1971). The rotation is not axisymmetric however, and in addition to rotation there are expansion motions of up to 100 km s^{-1} in position angles 68–120° and 248–278° (*cf.* Section 2.4 above). The motions of the stars in the nuclear region resemble the gas velocities (Rubin, Ford & Kumar 1973). Because of the age of the stars contributing to the spectra, Rubin *et al.* consider an explosive origin of the expansion motions to be unlikely, and tentatively suggest that we may be seeing part of ' a complex orbital motion '. Rubin & Ford (1971) have also noted that Lyngå (1959) found photographic evidence for a small central bar in position angle (pa) 85°, along the direction of expansion. A more extensive bar at pa $\approx 50°$ has been discussed by Lindblad (1956). Finally we mention that recent H I measurements, reported at the RGO Tercentenary Symposium by M. S. Roberts and by J. H. Oort, show non-circular motions along the minor axis of M31 which would correspond to contraction if they occur in the plane of the Galaxy.

M51 is another galaxy which has been well studied. Tully (1974) has made a detailed study of the kinematics of the inner region, and finds non-circular motions near the nucleus and streaming motions near the inner spiral arms, which he interprets in terms of a density wave with the inner Lindblad resonance at a radius of 600 pc. Within the resonance the gas motions are interpreted as elliptical dispersion orbits. Another galaxy of interest is NGC 4736, which contains a ring of H II regions at a distance of 2·4 kpc from the centre, and within this ring an unusual triple radio source, the middle component of which coincides with the nucleus (van der Kruit 1971b). Optical measurements show a smooth sinusoidal variation of velocity around the ring, except near the position angle of the triple radio source, where deviations of ± 60 km s^{-1} are observed (van der Kruit 1974). The velocity pattern over the remaining position angles is interpreted in terms of a rotating and expanding ring with parameters

$$a = 2{\cdot}4 \text{ kpc}, \quad V_R = 153 \text{ km s}^{-1}, \quad V_E = 28 \text{ km s}^{-1},$$

although, as van der Kruit remarks, a solution of pure rotation cannot be ruled out.

Evidence for a small contracting ring in the barred spiral galaxy NGC 3351 has recently been presented by Rubin, Ford & Peterson (1975). The ' nucleus ' of this galaxy consists of a ring of H II regions, whose velocities are interpreted in terms of a rotating and contracting ring with parameters

$$a = 340 \text{ pc}, \quad V_R = 126 \text{ km s}^{-1}, \quad V_E = -34 \text{ km s}^{-1}.$$

In general, barred spiral galaxies exhibit rapid rotation of gas in their nuclear regions together with non-circular motions of $\sim \pm 100$ km s^{-1}, of the same order as seen in the Galaxy (E. M. Burbidge 1970). It is not clear what kinematical connection there is between the rapidly rotating nuclear region and the barred structure. There is a similar problem in our own Galaxy in understanding the relationship between the nuclear disk and the expanding material. This will be considered in Paper IV of the series.

4. CONCLUSIONS

The distribution of high-velocity H I within $\sim 2{\cdot}5$ kpc of the centre is tilted at an angle of $9 \pm 4°$ to the plane of the Galaxy. Examples of this tilt in particular emission features have been noted by Kerr (1967), van der Kruit (1970), Sanders & Wrixon (1972a) and Kaifu *et al.* (1974), but the present work reveals clearly the three-dimensional nature of the tilt towards longitude $l = 124 \pm 28°$, and shows for the first time that the tilt is common to *all* the high-velocity emission (with $|V| > 50$ km s^{-1}). This discovery shows the need for extensive observations of molecular lines and hydrogen recombination lines away from the galactic plane, in order to determine whether the tilt is a general phenomenon. It also shows the importance of considering the regions above and below the plane, in addition to the plane itself, when modelling the inner region of the Galaxy. For example, the detailed model of the nuclear disk which Sanders & Wrixon (1973) constructed to fit their observations at $b = 0°$ should be re-examined in this light.

The kinematics of neutral hydrogen in the galactic centre have been summarized in Figs 3 and 4 (Section 2.4). The main points are the low rotational velocities of features lying out of the plane, decreasing towards the centre, and the high expansion velocities at all distances from the plane (within $|b| < 5°$), which increase towards the centre. There are marked deviations from axial symmetry in the velocity field (≈ 50 km s^{-1}), of the same order as those seen in external galaxies.

The expansion velocities seen near zero longitude can be explained either by an outflow of gas from the centre, or by the motion of gas in elliptical orbits. We emphasize that both possibilities are consistent with the present observations. In the case of outflow, the smooth variation of velocity with longitude for the individual features would suggest that smooth acceleration and braking processes are involved. It seems that continual expulsion confined to a small range of angles with the plane is required to explain the whole range of features observed. In the case of elliptical orbits, axial ratios of up to 3:1 are needed, with mean rotational velocities of ≈ 200 km s^{-1} and epicyclic velocities of up to 100 km s^{-1}. It is important to make *dynamical* calculations to see whether such orbits are consistent with a central bar and whether there is a dynamical explanation for the tilt observed in the gas distribution.

ACKNOWLEDGMENTS

We thank Drs A. Pedlar and M. J. Kesteven for helpful discussions, and Mrs A. M. Cohen for her careful reading of the manuscript. We also thank Professor J. H. Oort and Dr J. E. B. Ponsonby for helpful comments.

REFERENCES

Becklin, E. E. & Neugebauer, G., 1968. *Astrophys. J.*, **151,** 145.
Burbidge, E. M., 1970. *Comm. Astrophys. Space Phys.*, **II,** 25.
Burbidge, G. R., 1970. *A. Rev. Astr. Astrophys.*, **8,** 369.
Burke, B. F. & Tuve, M. A., 1963. *IAU Symp. No.* **20,** p. 183,eds F. J. Kerr, & A. W. Rodgers, Australian Academy of Science, Canberra.
Burton, W. B., 1970. *Astr. Astrophys. Suppl.*, **2,** 261.
Burton, W. B., 1971. *Astr. Astrophys.*, **10,** 76.
Burton, W. B. & Shane, W. W., 1970. *IAU Symp. No.* **38,** p. 397, eds W. Becker & G. Contopoulos, Reidel, Dordrecht, Holland.
Cohen, R. J., 1975. *Mon. Not. R. astr. Soc.*, **171,** 659.
Contopoulos, G., 1970. *Astrophys. J.*, **160,** 113.
Downes, D. & Maxwell, A., 1966. *Astrophys. J.*, **146,** 653.
Kaifu, N., Iguchi, T. & Kato, T., 1974. *Publ. astr. Soc. Japan,* **26,** 117.
Kerr, F. J., 1967. *IAU Symp. No.* **31,** p. 239, ed. van Woerden, H., Academic Press, London.
Kerr, F. J., 1969. *Aust. J. Phys., Astrophys. Suppl.*, **9.**
Kerr, F. J. & Sinclair, M. W., 1966. *Nature*, **212,** 166.
Kruit, P. C. van der, 1970. *Astr. Astrophys.*, **4,** 462.
Kruit, P. C. van der, 1971a. *Astr. Astrophys.*, **13,** 405.
Kruit, P. C. van der, 1971b. *Astr. Astrophys.*, **15,** 110.
Kruit, P. C. van der, 1974. *Astrophys. J.*, **188,** 3.
Kruit, P. C. van der, Oort, J. H. & Mathewson, D. S., 1972. *Astr. Astrophys.*, **21,** 169.
Lequeux, J., 1967. *IAU Symp. No.* **31,** p. 393, ed. H. van Woerden, Academic Press, London.
Lin, C. C. & Shu, F. H., 1967. *IAU Symp. No.* **31,** p. 313, ed. H. van Woerden, Academic Press, London.
Lindblad, B., 1956. *Stockholm Obs. Ann.*, **19,** No. 2.
Lyngå, G., 1959. *Medd. Lunds Astr. Obs*, Ser. II, No. 137.
Oort, J. H., 1964. *Trans. IAU*, **XIIA,** 789.
Parijsky, Y. N., 1963. *IAU Symp. No.* **20,** p. 172, eds F. J. Kerr & A. W. Rodgers, Australian Academy of Science, Canberra.
Peters, W. L., 1975. *Astrophys. J.*, **195,** 617.
Rougoor, G. W., 1964. *Bull. astr. Inst. Nethl.*, **17,** 381.
Rougoor, G. W. & Oort, J. H., 1960. *Proc. Nat. Acad. Sci.*, **46,** 1.
Rubin, V. C. & Ford, W. K., 1970. *Astrophys. J.*, **159,** 379.
Rubin, V. C. & Ford, W. K., 1971. *Astrophys. J.*, **170,** 25.
Rubin, V. C., Ford, W. K. & Kumar, C. K., 1973. *Astrophys. J.*, **181,** 61.
Rubin, V. C., Ford, W. K. & Peterson, C. J., 1975. *Astrophys. J.*, **199,** 39.
Sanders, R. H. & Wrixon, G. T., 1972a. *Astr. Astrophys.*, **18,** 92.
Sanders, R. H. & Wrixon, G. T., 1972b. *Astr. Astrophys.*, **18,** 467.
Sanders, R. H. & Wrixon, G. T., 1973. *Astr. Astrophys.*, **26,** 365.
Sanders, R. H., Wrixon, G. T. & Penzias, A. A., 1972. *Astr. Astrophys.*, **16,** 322.
Saraber, M. J. M. & Shane, W. W., 1974. *Astr. Astrophys.*, **36,** 365.
Shane, W. W., 1972. *Astr. Astrophys.*, **16,** 118.
Simonson, S. C., 1971. *Astr. Astrophys.*, **12,** 136.
Simonson, S. C. & Mader, G. L., 1973. *Astr. Astrophys.*, **27,** 337.
Tully, R. B., 1974. *Astrophys. J., Suppl. Ser.*, **27,** 415.

APPENDIX

In the light of more recent observations we have made the following change in nomenclature for the negative-velocity features XIV and XV described in Paper I (Cohen 1975). Feature XIV at $l = 355°$, $V = -220$ km s^{-1} we have relabelled XIVa. The adjacent feature at $V = -170$ km s^{-1} we have relabelled XIVb; this

feature was labelled XV in Paper I. The confusion in terminology arose because van der Kruit's l–V chart (van der Kruit 1970) shows a single feature, labelled XIV, at the mean velocity of XIVa and XIVb. More recent observations made at Jodrell Bank show XIVb to be quite distinct from van der Kruit's feature XV. XIVb continues past $l = 353°$ with a velocity of $V \simeq -176$ km s^{-1}, some 40 km s^{-1} more negative than the velocity of van der Kruit's feature XV at this longitude.

This change in terminology has been incorporated in the present paper.